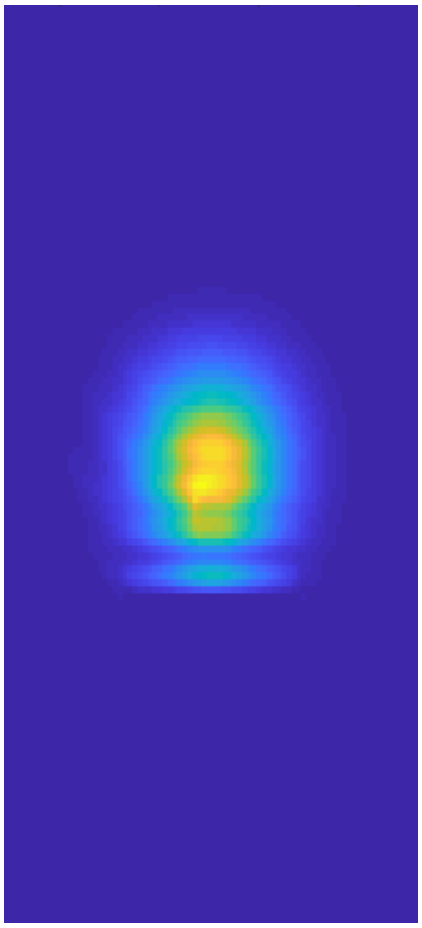

Quantum Tunneling and Quantum Reflection

Daniel Long | 14/12/2018

Abstract

A computational model has been constructed for evolving a quantum particle in one and two dimensions. With this model the evolution of the particle in the presence of various potentials has been analysed. The model was found to fit analytical solutions for a particle propagating in one dimension. The one-dimensional model also found transmission and reflection probabilities of particles of different energies, which fitted the analytical solution. Once the coefficients had been determined for a simple rectangular barrier, a double barrier was analysed. The coefficients were measured against the barrier separation. This analysis uncovered resonances in the boundary which affected the transmission. The two-dimensional model simulated the expected diffraction pattern when a particle was incident on a double slit structure. The two-dimensional model was also used to visualize quantum reflection on a negative barrier This report outlines the approach undertaken in building these models, as well as the results obtained when applying the model.

INTRODUCTION

Quantum tunneling and quantum reflection are prevalent in all quantum systems. Without tunneling, classical intuition would lead us astray. Classically, a particle needs enough energy to surpass a potential barrier; if the particle lacks the energy it will simply be reflected from the barrier.

In the early 20th century, the classical view of a particle was being contradicted by spurious results, particularly in nuclear physics. To explain these results, physicists such as Dirac and Oppenheimer developed the new field of quantum mechanics. In 1928, Oppenheimer published a key paper in which he discussed the aperiodic orbits of hydrogen [1]. Oppenheimer never explicitly referred to tunneling when discussing the ionization probability, however, in section three of his paper he showed how the classical view differed from the quantum view. Using the language of perturbation theory, Oppenheimer showed that, unlike the classical picture, with an electron's stationary state being localised, in the quantum picture an electron is free to escape the nucleus and, when subject to a field there will be a growing probability of escaping. This work was subsequently applied to various experiments with considerable success.

One early example of quantum tunneling being used to explain experimental data was research on alpha particle emission. In experiments, directed by Rutherford, it was found that low energy alpha particles were able to escape from the nucleus. However, if the nucleus was bombarded with alpha particles of a higher energy these alpha particles would not enter the nucleus. In 1928, George Gamow applied the recently developed quantum mechanics to resolve the observations. Quantum tunneling allowed the alpha particles to exist outside the classically forbidden region and therefore predicting alpha emission at the low temperatures seen experimentally [2].

Tunneling has since been used widely to develop modern technology such as flash memory storage- widely used in modern computing -and the scanning tunneling microscope. The scanning tunneling microscope has become an indispensable tool for research, one example of its use was in the 2016 imaging of cooper pairs in a superconductor [3]. Through utilising tunneling, researchers were able to produce evidence for behavior first predicted in 1964.

One starting point to deriving tunneling is the time independent Schrödinger equation,

$$\left[-\frac{\hbar^2}{2m}\frac{\partial^2}{\partial x^2}+V(x)\right]\psi(x)=E\psi(x) \qquad [1]$$

where $\psi(x)$ is the particle's wavefunction, m is the particle's mass, $V(x)$ is the potential at x and E is the energy of the particle.

For simplicity we will consider a rectangular potential, defined as

$$V(x)=\begin{cases}0, & x<-a\\ V_0, & -a<x<a\\ 0, & x>a\end{cases} \qquad [2]$$

where V_0 is the potential barrier's height and a defines the width of the barrier.

The general solutions to the Schrödinger equation in the presence of the potential is,

$$\psi(x)=\begin{cases}Ae^{ikx}+Be^{-ikx}, & x<-a\\ Ce^{qx}+De^{-qx}, & -a<x<a\\ Ee^{ikx}, & x>a\end{cases} \qquad [3]$$

where A, B, C, D, E are arbitrary amplitudes, k is a wavevector and q is a decay constant. They are defined as,

$$k=\frac{\sqrt{2mE}}{\hbar} \qquad [4]$$

$$\text{and,} \quad q=\frac{\sqrt{2m(V_0-E)}}{\hbar}. \qquad [5]$$

By applying the continuity condition for the wavefunction and it's first derivative at the boundaries of the potential, ratios of the amplitudes can be found. Through taking the ratio of the outgoing amplitude and the incident amplitude, the following expressions for the transmission probability can be found,

$$T = \frac{1}{1 + \frac{{V_0}^2}{4E(V_0 - E)} sinh^2\left(\frac{2a}{\hbar}\sqrt{2m(V_0 - E)}\right)}$$

[7]

A full derivation of the transmission probability can be found in Manogue et al. [4]

A plot of the transmission probability can be seen in figure 1 below. The reflection probability is also plotted in figure 1. The reflection probability can be found by subtracting the transmission probability from one.

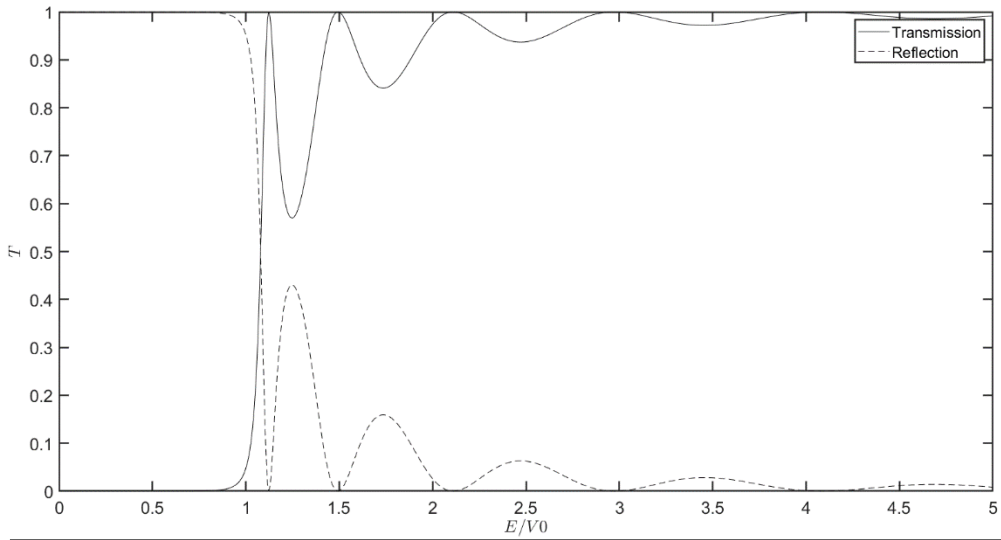

Figure 1: A graph of the expected transmission and reflection probabilities with respect to the particle energy

The $sinh^2$ term in the denominator of equation 6 induces the oscillations in the probabilities. This oscillation arises from the wave emerging from the potential with a certain phase, dependent on the wavelength of the incident wave and the barrier gap.

One aim of this investigation is to verify this analytical solution in figure 1, through finding agreement with simulation. It is important to note that the analytical solution considers a monochromatic wave packet. In the simulation it is not feasible to use a monochromatic wave packet, therefore, it will not be possible to reproduce figure one. However, it should be possible to produce the expected behavior. Once the model is

known to be accurate, the behavior of a wave packet in the presence of a double barrier will be investigated.

The second aim will be to reproduce the expected interference pattern in a double slit experiment. This will require building a two-dimensional model for a quantum particle. The double slit experiment was central to the development of quantum mechanics as it demonstrated clear evidence for the wave like nature of matter. Reproducing the interference pattern will demonstrate the accuracy of the two-dimensional simulation. Further study will then be performed with the two-dimensional simulation on a region with a negative potential. It is expected that quantum reflection (as well as some trapping and transmission) will occur in the presence of the negative potential.

Model

The first step to modelling quantum reflection is to define the region in which a particle and a barrier will be simulated. The simulated region must be large enough so as to not alias the wavefunction and to correctly simulate the system, however, the larger the system the longer it will take to be simulated. Once the region is defined the next step is to define the initial wavefunction. To do this a gaussian wave packet was used, given by,

$$\psi(x, t = 0) = \frac{e^{\frac{-(x-x_0)^2}{4\sigma^2}}}{(2\pi)^{\frac{1}{4}}\sqrt{\sigma}} e^{ik_0 x}$$

[8]

where $\psi(x, t = 0)$ is the initial state of the wavefunction, x_0 is the centre of the wave packet, σ is the width of the wave packet and k_0 is the wave number. It is useful to note that the wave number, k_0, relates to the mean momentum of particle in the state through,

$$\bar{p} = \hbar k_0$$

[9]

where $\bar{p}$ is the mean momentum. It is also useful to note that the wave number relates to the particle's energy through

$$E = \frac{\hbar k_0}{2m}$$

[10]

where E is the particle's energy and m is the mass of the particle.

Through setting the constants appropriately for the chosen simulated region, a particle can be plotted in its initial state. It is convenient to set the constants to unity as this will lead to an easily visualised wave packet.

To propagate the wavefunction the time dependent Schrödinger equation is used,

$$i\hbar\frac{\partial}{\partial t}\psi(x,t) = -\frac{\hbar^2}{2m}\frac{\partial^2}{\partial x^2}\psi(x,t) + V(x)\psi(x,t).$$

[11]

When solving this equation numerically we divide up the wavefunction into the grid of our region and store it as a vector of dimension $N \times 1$. When applying the potential and the second order differential operator we can use matrix multiplication. The simplest of the two matrices is the potential. As seen in equation 9, the potential at each location is to be multiplied by the wavefunction. We can do this by creating a vector of the potential of size $N \times 1$, this vector will then be transformed into an identity matrix of size $N \times N$, such that the potential vector lies along the diagonal of the matrix. When this matrix is applied to the wavefunction it will create a vector of size $N \times 1$, which is the desired product.

The more complex case is the second order differential operator. This operator can be approximated using,

$$\frac{\partial^2}{\partial x^2}\psi(x,t) \rightarrow \frac{\psi(x_{n-1},t) - 2\psi(x_n,t) + \psi(x_{n+1},t)}{(\Delta x)^2}$$

[12]

where $\psi(x_{n-1},t)$ is the value of the wavefunction at the preceding simulated point, $\psi(x_{n+1},t)$ is the value of the wavefunction at the subsequent simulated point and Δx is the spacing between simulated points. An efficient way of computing this approximation is by creating an $N \times N$ matrix. In the leading diagonal there will be a minus two, divided by the interval spacing squared. On the diagonals neighboring the leading diagonal there will be a one, also divided by the interval spacing squared. When this matrix is applied to the wavefunction it will creating an $N \times 1$ vector with the nth value given by equation 10. This approximation to the differential operator is valid if the interval spacing is much less than one. Ideally the spacing should be of the order 10^{-3}.

With equation 10 expressed in matrix form a differential equation solver can be used to numerically propagate the wavefunction in time. In this project both a built-in differential equation solver and a user-built function was used. It was found that certain tasks, such as 1D wave propagation, were faster when done by a built-in differential equation solver, whereas in the 2D case the user-built differential equation solver was faster.

The user-built differential equation solver used the Runge-Kutta method. This method approximates the function by taking small steps, in this case in time. the value at the next

time step is given by the gradient at the midpoint of the time step, extended the distance of the time step. The quality of the approximation is dependent on the size of the timestep, however too small a timestep results in a much slower simulation.

When solving the differential equation many iterations of the matrix multiplications are performed. These multiplications are slow as the matrices are large, $N \times N$, in size. By converting the matrices into sparse matrices, the calculations can be performed much faster. Another way to speed up the iterations was to round the initial wave packets elements to roughly 12 significant figures. This meant that the fine detail in the wave packet was lost, however this detail was not important in the propagation of the wavefunction.

Once propagation is implemented the simulation can be tested against an analytical solution. The analytical solution used to verify the code in this project was a free wave packet, whose propagation was determined using the result given in Schwabl's Quantum Mechanics textbook [5]. A video of this confirmation can be seen under the title, AnalyticTestProbability.gif. In the video the simulated solution is plotted using blue dots, the analytical solution is plotted with a black dashed line. It is evident in the gif that the simulation correctly models the propagation of the probability distributions.

Previously the wavefunction has been propagating in the absence of a potential. In order to analyse quantum tunneling and reflection a potential is needed. The simplest potential to consider is a square potential. In figure 2 the transmission and reflection probabilities are plotted against the particle energy. These plots show that a low energy particle has a very low probability of tunneling, however this probability rapidly increases as the particle energy approaches the potential of the box. In order to demonstrate the correlation with the expected relation, shown in figure 1, the plots show the effect of increasing σ, the width of the wave packet. As the wave packet widens in real space the wave packet narrows in k-space, this makes the simulation a better approximation for the case of a monochromatic source. It was not possible to increase the width indefinitely as it is unfeasible to display too wide a wave packet in the limited region. This approximation can be thought of as a convolution of figure 1, when sigma is small the analytical solution has been heavily smoothed by a convolution and therefore the peaks will not be clearly seen.

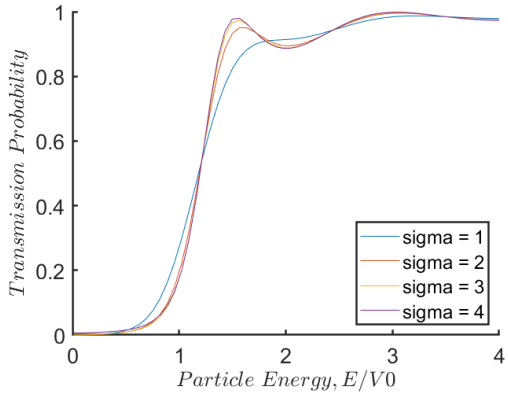

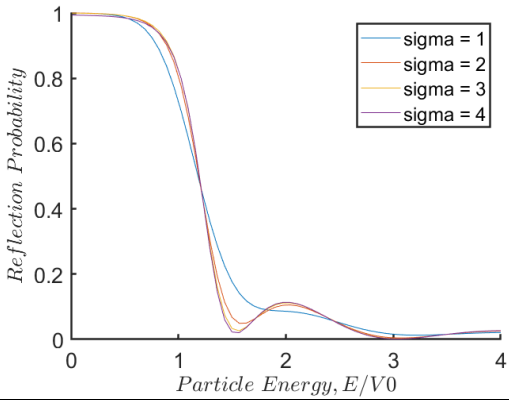

Figures 2 and 3: The transmission and reflection probabilities of a particle incident on a rectangular potential, against the energy of the particle, scaled by the magnitude of the

Once the programme had proven to produce accurate data for the 1D case, the model was extended to two dimensions. Modelling the particle in two dimensions poses many problems, the key problem being the increase in the number of calculations required. In 2D the differential equation operator is of the size $N^2 \times N^2$, this means the gird size must be small, otherwise the matrices will become too large to calculate. The same approximation, as seen in equation 10, was used. To apply this approximation to the wavefunction in both the x and y direction an $N^2 \times 1$ vector was created. Through carefully constructing the matrix operators the approximation could be efficiently applied. A video of a particle propagating in 2D is found under 2Dparticle.gif. This video shows the simulation acting as expected, with a particle's probability distribution travelling with a constant velocity and gradually spreading out. This animation is similar to the wavefunction shown in the video, AnalyticTestProbability.gif, except the 1D case is a slice of the 2D video.

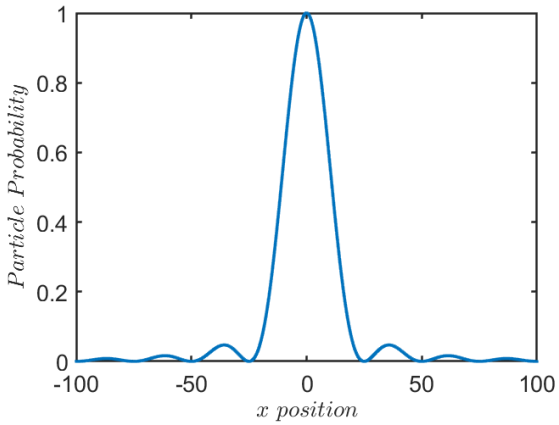

Figure 4: A plot of the expected double slit diffraction pattern

The 2D model was used to analyse the diffraction pattern of a particle incident on a screen with two, three and five slits. Figure 3 shows the expected diffraction pattern created by a beam of monochromatic light passing through a double slit. This same pattern is expected when a particle passes through a sufficiently narrow slit.

A full derivation and more detailed discussion of double slit diffraction can be found in Optics by Möller [6].

The simulation was run in 2D and a slice of the probability distribution halfway from the double slit barrier and the end of the window was plotted. The diffraction pattern begins to emerge once the particle has passed through the slits and becomes greatest when the particle is approaching the edge of the window. In figure 4 the measured diffraction pattern is shown. This pattern shows correspondence with the form of figure 3. The major discrepancies between the expected pattern and the simulated pattern is the lack in further peaks.

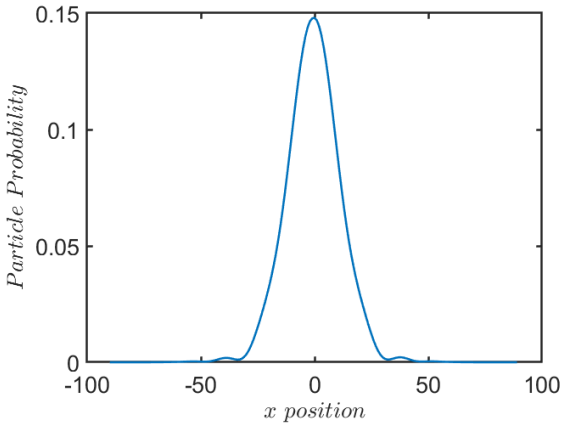

Figure 5: A plot of the simulated double slit diffraction pattern

The most probable cause of the lack of further peaks is that the simulation is not of high enough resolution, however with the computational resources available it was not possible to get a higher resolution.

A video of the particle passing through the double slit can be found saved as, 2DparticleDoubleSlit.gif.

SCIENTIFIC APPLICATION

Previously the model has been used to verify known results. This was primarily to test the model so that further study could be done on new concepts. One phenomenon that was studied was the transmission and reflection probabilities due to two barriers separated by a gap. It is expected that there will be resonance at certain barrier separations. The resonance is seen in below in figures 6 and 7, which show how the profiles of the transmission and reflection probabilities vary with the barrier separation. It is clear to see from the figures that separations which are multiples of each other have very similar profiles. The even separations follow almost the same profile, except for the case of zero separation. The zero separation is simply the $\sigma = 1$ case in figures 2 and 3. To understand the resonances in the coefficients it is important to remember that the energy corresponds to the wavenumber, k_0, of the wave packet. When the wavenumber is at a value that corresponds to a wavelength that perfectly fits inside the separation, there will be very

strong constructive interference. The strong constructive interference leads to a higher transmission probability at these points of coherence.

While it is expected that multiples of the same separation to have identical profiles- the region between has no potential so should not affect the transmission -this is not seen in the data. The likely cause for this variance is that the simulation has a finite sample size. Therefore, the grid will not fit perfectly inside the separation. This will cause the exact profile to vary with slit separation, this variance will be very small whilst the grid spacing is small.

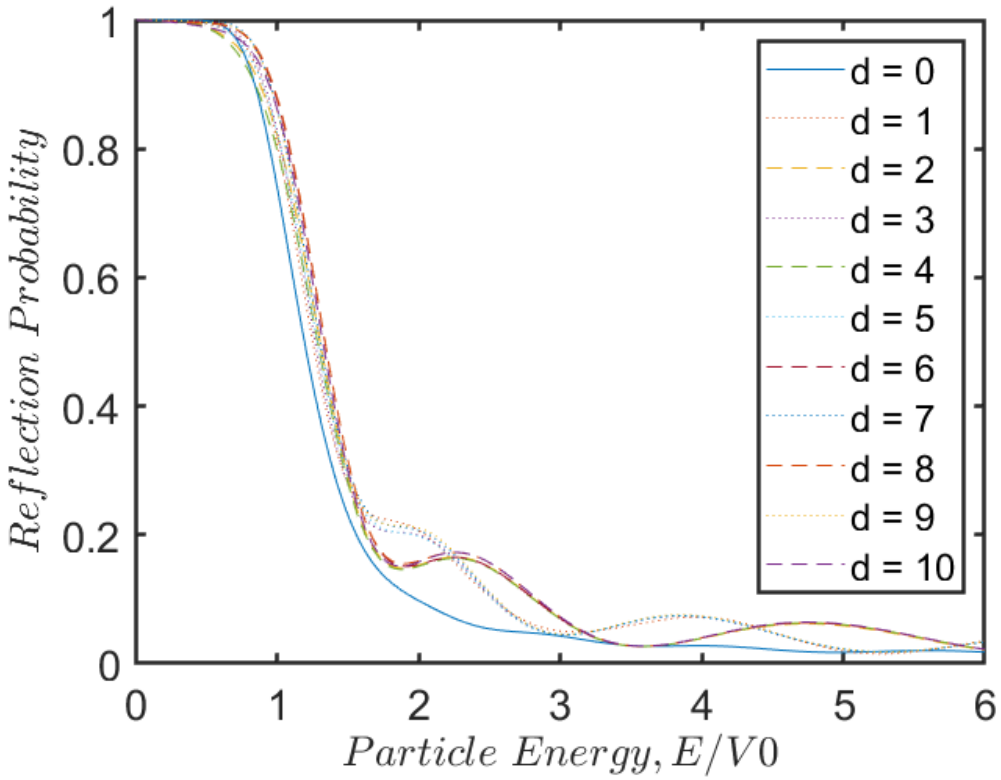

Figure 6: The transmission probability of a particle incident on two rectangular potentials separated by a distance d, against the energy of the particle, scaled by the magnitude of the potential.

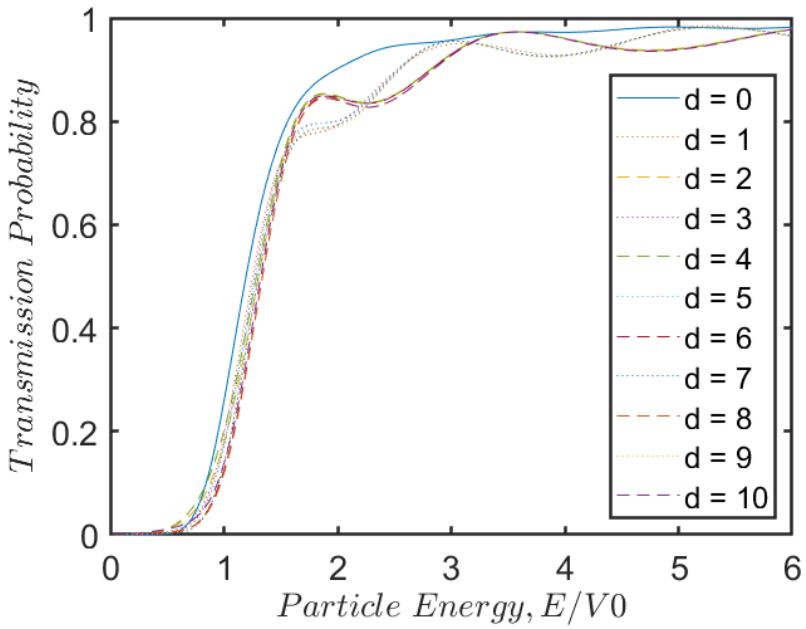

Figure 7: The Reflection probability of a particle incident on two rectangular potentials separated by a distance d, against the energy of the particle, scaled by the magnitude of the potential.

So far only positive potentials have been considered, in this section the behavior of a particle around a negative potential will be discussed. Using the two-dimensional model, a particle was propagated through a region of negative potential. This situation has three possible outcomes, the first is that the particle is reflected from the region of lower potential, the second is the particle being trapped in the region and the third is the particle passing through the region. All three of these outcomes can occur simultaneously, with the wavefunction splitting accordingly. To demonstrate these outcomes five videos are saved under: QuantumReflection.gif, QuantumReflectionAndTrapping.gif, QuantumTrapping.gif, PassingThrough.gif and QuantumReflectionTrappingPassing.gif. To simulate these situations a central square of negative potential was created. If the negative potential was close to zero, then the particle could pass over the region with little disturbance. This behavior occurred when the particle energy was in the region $0.2 < \frac{E}{|V_0|}$. A more negative potential would result in the particle being partially reflected, partially trapped and partially transmitted. Once $\frac{E}{|V_0|} < 0.05$ the particle will be almost entirely reflected.

SUMMARY

This model of a quantum particle has proved accurate and useful. In one dimension it was feasible to run a particle at many different energies and see how that affected its behavior when it encountered barriers of various forms. The one-dimensional model was used to find the dependence of the transmission and reflection probabilities on the particle energy. The simulation found that the tunneling probability was dependent on the energy of the wave packet, as well as the width of the wave packet. As the particle's energy approaches the potential of the barrier, the transmission probability begins increasing at approximately $E = V_0/2$. This transmission is due to quantum tunneling as it would not classically be allowed. The transmission probability increases until it approaches 1, at which point, depending on the width of the wave packet, there is oscillation in the probability, which gradually decreases in amplitude.

The one-dimensional simulation was also applied to the case of a double barrier. The simulation showed that a particle incident on a double barrier behaves much in the same way as when incident on a single barrier, except for the resonance found in the gap. To analyse the resonance, the separation between the barriers was varied. This model produced clear differences in the transmission vs particle energy profile between gaps with 'even' separations and 'odd' separations. This was clear evidence of resonance in the gap between barriers.

In two dimensions the computational work required to simulate even a relatively simple model was much higher. Therefore, the two-dimensional model was used for one-off simulations. The two-dimensional model was first used to reproduce the double slit interference pattern. This proved hard to simulate as the gird size was limited by the computational resources. An interference pattern was produced; however it did not show the full behavior expected.

With the two-dimensional model the phenomenon of quantum reflection was visualised. The dependence on particle energy for quantum reflection was found using the model and videos were created showing the different outcomes of a particle incident on a region of negative potential.

Further study could be performed with this simulation on the phenomenon of quantum reflection. However, work would need to be done to improve the simulation's resolution and speed as these areas limit any data accuracy and data collection. To speed up the code one could use a cluster of high-performance CPUs, solving the differential equation is a very linear algorithm and therefore could not be easily parallelized, however using a cluster would allow data to be collected on the effect of varying the initial conditions. A high-performance CPU would be needed to increase the resolution as the issue is the memory required to manipulate such large matrices which scale in system size by N^4. One of the first areas of study would then be to reproduce the dependence of the transmission and reflection probabilities on the particle energy in two dimensions.

REFERENCES

[1] Oppenheimer, J. (1928). Three notes on the quantum theory of aperiodic effects. Physical Review, 31(1), pages 66-81.

[2] G. Gamow, Z. Phys. 51, 204 (1928)

[3] M. H. Hamidian, S. D. Edkins, Sang Hyun Joo, A. Kostin, H. Eisaki, S. Uchida, M. J. Lawler, E.-A. Kim, A. P. Mackenzie, K. Fujita, Jinho Lee, J. C. Séamus Davis. Detection of a Cooper-pair density wave in Bi2Sr2CaCu2O8 x. Nature, 2016; DOI: 10.1038/nature17411

[4] McIntyre, H., Manogue C. A. & Tate, J., (2014). Quantum Mechanics. Pearson, pages 200-208.

[5] F. Schwabl, Quantum Mechanics, 4th ed, Springer (2007), page 17

[6] Möller K. D., Optics, University Science Books (1988), pages 138-141